Bioconvection and front formation of *Paramecium tetraurelia*

So Kitsunezaki*
Department of Physics, Graduate School of Human Culture, Nara Women's University, Nara 630-8506, Japan

Rie Komori
Department of Pharmaceutical Technology, Faculty of Pharmaceutical Sciences at Kagawa Campus, Tokushima Bunri University, Shido, Kagawa 769-2193, Japan

Terue Harumoto
Department of Biological Sciences, Faculty of Science, Nara Women's University, Nara 630-8506, Japan
(Received 23 August 2006; revised manuscript received 1 April 2007; published 2 October 2007)

We have investigated the bioconvection of *Paramecium tetraurelia* in high-density suspensions made by centrifugal concentration. When a suspension is kept at rest in a Hele-Shaw cell, a crowded front of paramecia is formed in the vicinity of the bottom and it propagates gradually toward the water-air interface. Fluid convection occurs under this front, and it is driven persistently by the upward swimming of paramecia. The roll structures of the bioconvection become turbulent with an increase in the depth of the suspension; they also change rapidly as the density of paramecia increases. Our experimental results suggest that lack of oxygen in the suspension causes the active individual motions of paramecia to induce the formation of this front.

DOI: 10.1103/PhysRevE.76.046301 PACS number(s): 47.63.Gd, 47.54.−r, 87.17.Jj, 87.18.Hf

I. INTRODUCTION

In suspensions of microorganisms, the self-propelling motion of living organisms often drives the density distribution to states that are hydrostatically unstable under gravity and persistent fluid convection is induced. This type of fluid convection is termed bioconvection. It has been observed in many types of protozoa and bacteria, such as *Tetrahymena pyriformis, Chlamydomonas nivalis, Bacillus subtilis, Heterosigma akashiwo*, and *Desulfovibrio desulfuricans* [1–7]. In typical cases, each individual is slightly denser than the ambient fluid and the upward motion of microorganisms leads to the formation of a high-density layer beneath the water surface. Fluid convection develops through a mechanism analogous to that of the Rayleigh-Taylor (RT) instability because the suspension in the layer has a higher specific gravity than that below [8–12].

Such upward motion is induced in the swimming response of microorganisms by certain stimuli. The stimulus responsible for bioconvection depends on the type of organism. Negative gravitaxis is the response of swimming in the opposite direction to gravity. Some microorganisms such as *Loxodes* and *Euglena* are believed to sense the direction of gravity physiologically [13–19], while the mechanism is considered to be purely physical in some cases. Gyrotaxis is a process in which the swimming direction of each individual is determined by the balance of external and viscous torques [11,20–25]. A bottom-heavy microorganism may swim upward in still water due to gyrotaxis. Phototaxis (or photokinesis) and oxykinesis are the responses of swimming toward light or along oxygen gradients.[1] These can also cause upward swimming under appropriate conditions [3,4,6,26,27].

Some continuum models have been proposed for bioconvection. These models are constructed from the Navier-Stokes equation and a transport equation describing diffusion, self-propelled motion, and advection. They have been investigated using linear or weak-nonlinear analysis and numerical simulations [8–12,23–25,28–37]. These models successfully describe bioconvection phenomena as the result of the interaction between the densities of the microorganism and the fluid. However, cell-cell interactions such as collisions and biological intercellular communication become considerably more important in concentrated suspensions. Bioconvection may be considered as a sort of collective motion in such situations [12,38–44].

We report experimental results on bioconvection by *Paramecium tetraurelia* in high-density suspensions obtained by centrifugal concentration. As per our understanding, the bioconvection of *Paramecia* has not been investigated thoroughly. We observed that bioconvection by *P. tetraurelia* begins with the propagation of a high-density front from the bottom of a suspension toward the surface [45]. Such front propagation does not appear in typical bioconvection phenomena. In the present study, we focus on front propagation to clarify the mechanism inducing bioconvection by *P. tetraurelia*.

P. tetraurelia is a cigar-shaped ciliate with a length of 90–170 μm, and its mass density is slightly higher than that of water. *Paramecia* are known to exhibit responses to various stimuli, such as thermokinesis, chemokinesis, glavanotaxis, gyrotaxis, and gravitaxis [13,16–19,22,46–50]. They

*kitsune@ki-rin.phys.nara-wu.ac.jp;
URL: http://www.complex.phys.nara-wu.ac.jp/~kitsune

[1]We distinguish between "taxis" and "kinesis" depending on whether an individual swims by sensing the direction of a stimulus or not [50].

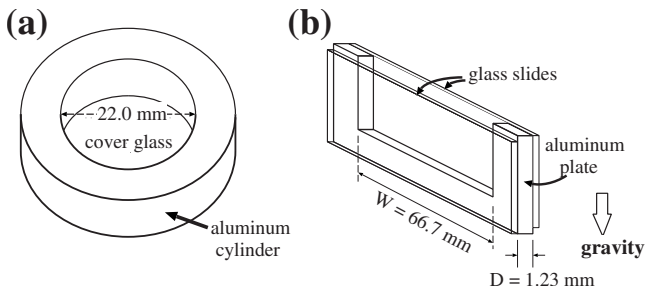

FIG. 1. Schematic diagrams of the containers of a suspension. (a) A cylindrical container and (b) a Hele-Shaw cell placed vertically.

behave diffusively in normal density suspensions because they swim backward after collisions with other individuals to avoid contact with them. However, we observed that paramecia in high-density suspensions made by centrifugal concentration form a crowded front to produce bioconvection, as reported in Secs. II and III. In experiments on quasi-two-dimensional bioconvection using Hele-Shaw cells, we find that a high-density front of *P. tetraurelia* appears in the vicinity of the bottom and propagates gradually toward the surface. Bioconvection occurs with this propagation and remains after the front stops beneath the surface. In Sec. IV, we report the movement of paramecia and the time development of the bioconvection patterns. The roll structures of bioconvection developing under the front are not stationary when the depth of the suspension is large. In order to investigate the effect of oxygen, we conducted experiments in a nitrogen environment. The front and the bioconvection of *P. tetraurelia* disappear when the air is replaced with nitrogen gas, and *P. tetraurelia* swim more actively in a nitrogen environment than in air (see Sec. V). These results suggest that lack of oxygen dissolved in the suspension causes the active individual motions of *P. tetraurelia* to induce front formation.

II. EXPERIMENTAL METHODS

We used *P. tetraurelia* multiplied by cloning from wild-type stock 51 to ensure genetic uniformity. Before each experiment we grew the paramecia in culture containing bacteria as feed[2] at 25 °C for 3–4 days. We then prepared a 400-ml suspension of paramecia. The density of paramecia was approximately 10^3 cells/ml in this suspension and could not increase further because it was in the stationary phase of cell growth [51–53].

This suspension was strained through gauze and concentrated by centrifugation performed twice. The second centrifugation was performed after transferring the sediment obtained in the first to approximately 100 ml of the synthetic solution SMBIII [54] and the resulting sediment was filtered again. We finally obtained an approximately 1-ml suspension containing paramecia with a density of the order of 10^5 cells/ml. The suspension did not contain food for paramecia because the bacteria were eliminated with the solution remaining after the first centrifugation and the SMBIII contained no food. Lower-density suspensions were obtained by diluting with SMBIII.

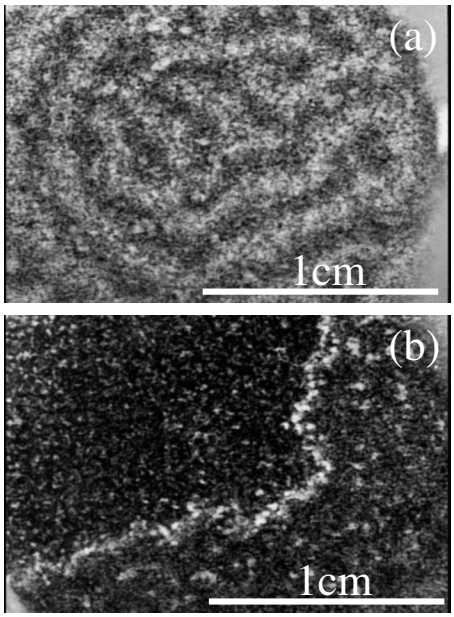

FIG. 2. Bioconvection patterns in suspensions of $V=1.00$ ml ($H \simeq 2.6$ mm) at $T=25\pm0.5$ °C. (a) $n_0=5.8\pm0.9$ (10^5 cells/ml) and (b) $n_0=2.9\pm0.5$ (10^5 cells/ml).

To determine the density of paramecia in the suspension, n_0, we made 15 samples of 5 μl from a part of the suspension diluted by 1/40. The number of paramecia in each sample was determined using a stereomicroscope. The density n_0 was calculated from the average of 11 data points obtained by discarding the two largest and the two smallest values from the 15 data points. The experiments were conducted within half a day of the centrifugations and density measurement. Almost every paramecium maintained its activity during each experiment. The number of paramecia was effectively constant because they could not increase in the suspensions.

In each experiment, we kept the suspension at rest after stirring in order to create a uniform state from the start. The main control parameters were the volume of the suspension V, which determined the depth of the suspension, H in the containers, and n_0. V was measured with an accuracy of 1% using a micropipette. The temperature T of the suspension was maintained constant. The containers were made of aluminum and glass to maintain the temperature in the suspension as uniform as possible.

We used both a cylindrical container and Hele-Shaw cells as shown in Fig. 1. The cylindrical container was composed of an aluminum wall and a cover glass bottom. Its inner diameter was 22.0 mm. The container was placed horizontally, and the bioconvection patterns in it were observed un-

[2]0.5% phosphate-buffered wheat grass powder (Pines Int., Inc., Lawrence, KS) infusion supplemented with 0.5 mg/l stigmasterol and inoculated with *Enterobacter aerogenes* or *Klebsiella pneumoniae* 2–3 days before use. The latter bacteria were used in our early experiments including those in Fig. 2. We have observed no effect on bioconvection due to the type of bacteria used.

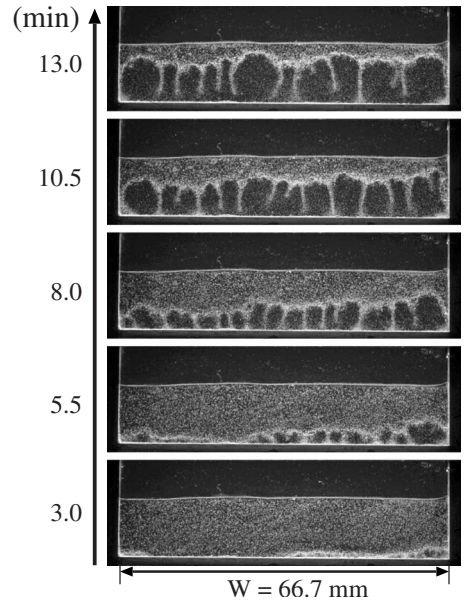

FIG. 3. Formation of a bioconvection pattern in the Hele-Shaw cell. A suspension of $V=1.00$ ml and $n_0=0.61\pm0.22$ (10^5 cells/ml) was used. Time after stirring is shown on the left of each photograph.

der a stereomicroscope (Leica MS-5). The container was dipped into a constant-temperature water bath regulated by a temperature controller. The Hele-Shaw cells were constructed from two parallel glass slides that are geometrically identical and have an inner thickness of $D=1.23\pm0.05$ mm and an inner width of $W=66.7\pm0.1$ mm. Thin stainless-steel wires were used for stirring the suspension. The cells were placed in an environment maintained at a temperature of 27 ± 1 °C by an air conditioner. Images of the patterns were taken with a digital camera (Canon EOS10D) using an interval timer. The individual motions of paramecia were observed under another stereomicroscope (Wraymer SW-700TD).

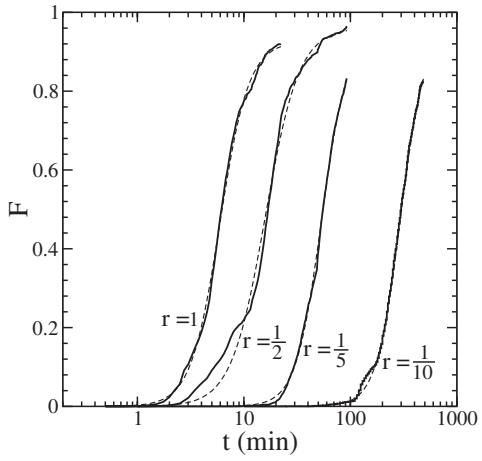

FIG. 4. Time development of the area swept by a front, $F(t)$, for suspensions with $V=1.00$ ml and $n_0=(1.9\pm0.3)r$ (10^5 cells/ml), where r is the dilution ratio of the suspension used. The results are well fitted by the function $a/\{1+(\tau/t)^c\}$ indicated by the dotted lines.

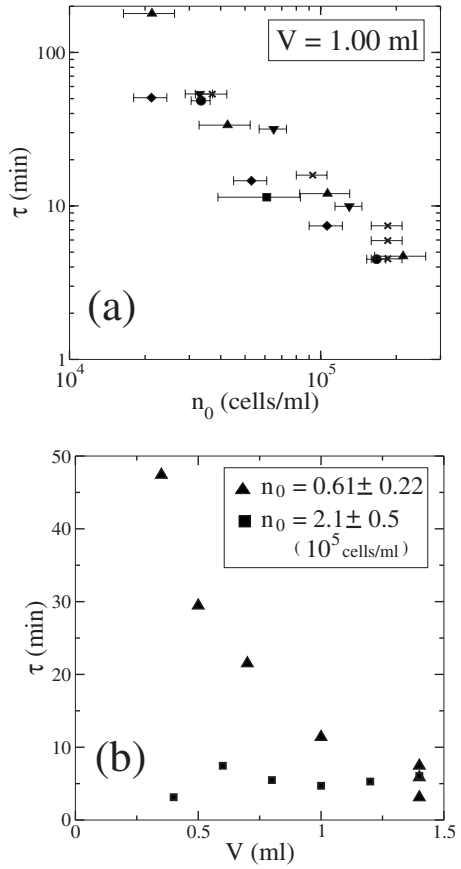

FIG. 5. Dependence of τ on (a) n_0 for a fixed volume and (b) V for two different densities. Data obtained from the same culture are plotted with a common symbol. The error bars represent the standard deviations for the measurements of n_0.

The containers were illuminated uniformly from behind; the oblique light of the stereomicroscopes was used for the cylindrical container and a light box including a 2-W white light-emitting-diode (LED) lamp for the Hele-Shaw cells. The Hele-Shaw cells were illuminated with diffused light at about 150 lux in the experiments reported here. The bioconvection also appears under daylight which is rather bright compared with this light condition. The dense regions of paramecia appear white in our images because paramecia scatter light. The digital images from the stereomicroscopes were recorded through a charge-coupled device (CCD) using a video camera (Sony DCR-PC100).

We performed several preliminary experiments before settling on the containers described above. We tried a glass Petri dish and a Hele-Shaw cell made of acrylic instead of aluminum and tested two types of adhesives—epoxy and paraffin—to join the aluminum wall and the glass plates. The phenomena reported in this paper were observed in all these cases. Therefore, we believe that the container materials did not affect the behavior of paramecia. The effect of evaporation was also not important because it was negligibly small under our experimental conditions. In fact, the bioconvection patterns did not change even when we covered the cylindri-

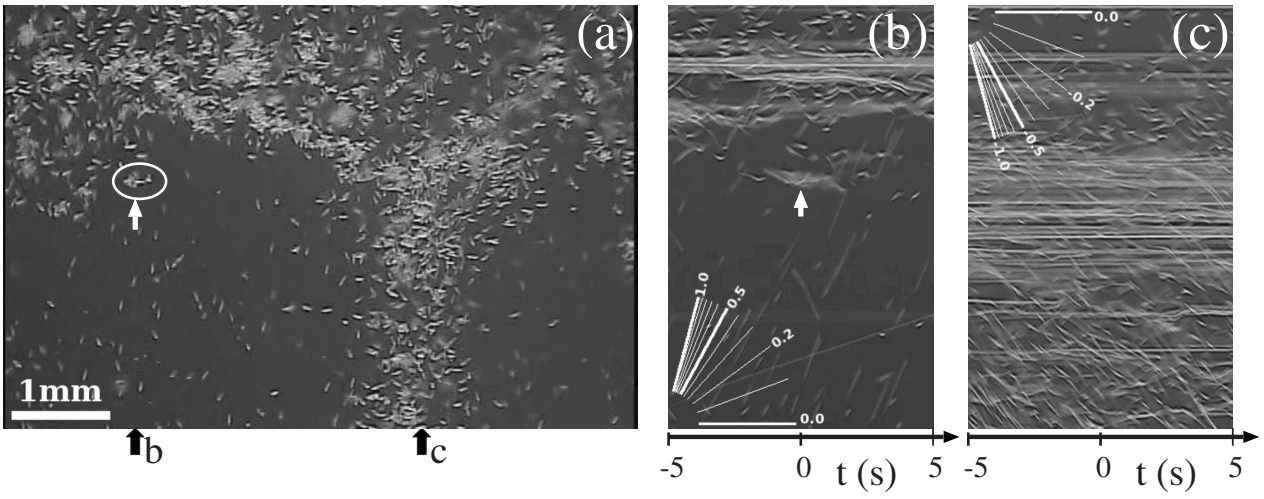

FIG. 6. (a) A microscopic image of a front in a suspension with $n_0=0.95\pm0.13$ (10^5 cells/ml) and $V=1.00$ ml. Individual paramecia appear as white specks. (b) and (c) Space-time plots of vertical slices at positions indicated by black arrows in (a). The abscissa axis represents time, where (a) is obtained at $t=0$. White radial lines with numeric values represent the scales of velocities (mm/s). White arrows in (a) and (b) indicate a cluster disassembling in the upward flow.

cal container with a lid or placed the containers in a closed box.

III. FORMATION OF BIOCONVECTION PATTERNS OF *P. TETRAURELIA*

A. Patterns in the cylindrical container

Figure 2 shows photographs of the bioconvection patterns of *P. tetraurelia* appearing in the cylindrical container. These photographs show the top view of the containers 12 min after stirring. The top surface of the suspension was open to the air, and it was almost horizontal, although it was slightly high in the vicinity of the wall due to surface tension. When the density is high, the bioconvection patterns appear a few minutes after initial stirring. As shown in Fig. 2(a), the width of a roll is of the same order as the depth of the suspension, although the roll structures do not become stationary. These bioconvection patterns are insensitive to temperature variation in the range 25–30 °C.

The density of paramecia in Fig. 2(b) is half that in Fig. 2(a). As n_0 decreases, the formation of the roll structures takes a longer time and the structure becomes less pronounced. In such cases, the bioconvection patterns often appear with the propagation of a front composed of aggregated paramecia, as shown in Fig. 2(b). For small values of H, the front cannot cover the center region and the bioconvection pattern appears only in the vicinity of the wall.

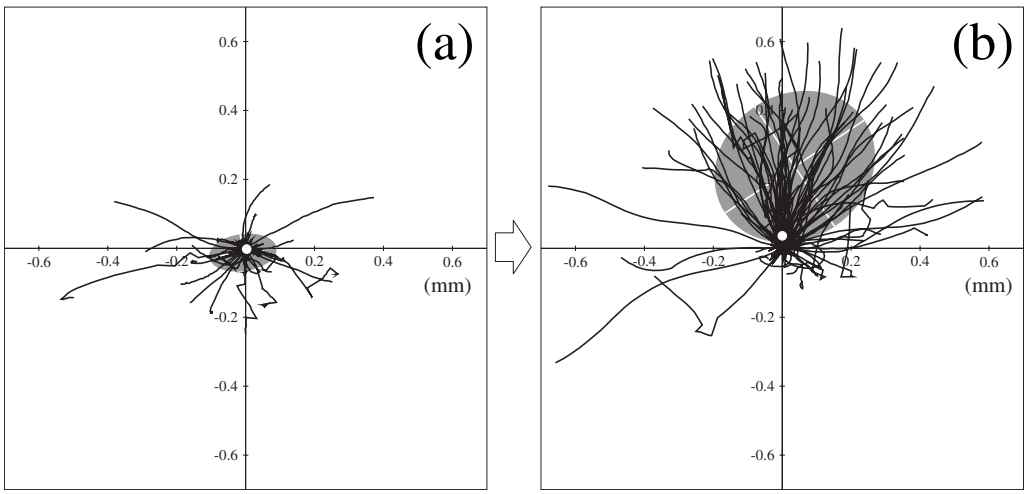

FIG. 7. Individual trajectories of 100 paramecia for 1 s (a) before and (b) after the passage of the front. This observation point was placed in an upward flow after the passage of the front. The gray ellipse represents the covariance ellipse of these displacements, and the small white circle indicates the displacement of the ambient fluid estimated from the movements of small, passive, suspended particles.

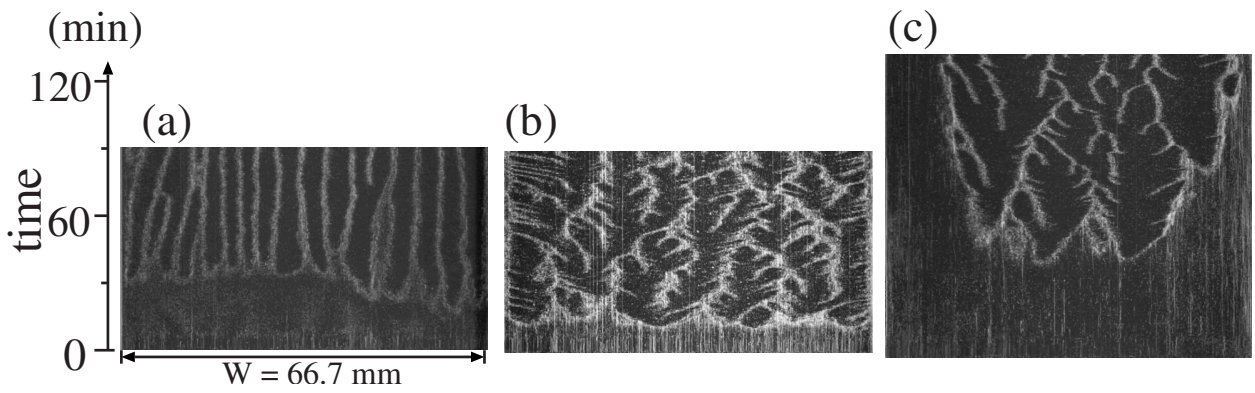

FIG. 8. Space-time plots of horizontal slices at a fixed height. The suspensions in (a) and (b) have the same density $n_0=0.61\pm0.22$ (10^5 cells/ml), but different volumes: (a) $V=0.50$ ml and (b) $V=1.00$ ml. The suspension in (c) has the same volume as that in (b) but density $n_0=0.21\pm0.03$ (10^5 cells/ml). Heights of $y=0.5H$ (a),(c) and $y=0.75H$ (b) are used to show the patterns clearly.

B. Front formation in the Hele-Shaw cell

We investigated the formation process of the convection patterns by using the Hele-Shaw cells as containers. Fluid flows in the containers are quasi-two-dimensional flows, although the inner thickness D is much larger than the length of a paramecium. The containers were placed so that the walls were vertical, and photographs were taken horizontally. The top surface of the suspension was open to the air. The surface was made as horizontal as possible at the time of stirring although it often remained uneven due to the surface tension between the suspension and the walls of the cell.

Figure 3 shows the formation of bioconvection in the Hele-Shaw cell through a series of photographs. Initially, no oriented swimming is observed in the uniform suspension of *P. tetraurelia*. After about 5 min, a dense front of paramecia is formed in the vicinity of the bottom of the cell. The front propagates toward the top surface, increasing the size of the fluid convection cell below it. In suspensions with a low density or small volume, the front first appears only in part of the bottom of the cell and then gradually spreads over the entire width as the front propagates upward. Front propagation is not observed in typical bioconvection phenomena because the taxis or kinesis property of the microorganisms causes individuals to swim upward at the outset to form a high-density layer beneath the top surface.

Both the formation time and the propagation speed of the front depend significantly on n_0 and V. In order to investigate the front propagation quantitatively, we measured the proportion of the area swept by the front, $F(t)$. The series of digital images in each experiment were obtained at constant time intervals of $\Delta t=0.25-5.00$ min after stirring. The area swept by the front at a given time $t=n\Delta t$ was determined from the region where the brightness varied significantly between the initial and nth images. For this estimation, the following procedure was employed. (i) We cropped a rectangular region with a size of $(3/5)W\times H$ in the center of each image and calculated the brightness $b_i(x,y)$ at the position (x,y) in the ith cropped image as the neighborhood mean in an area of 2.0 mm $\times$ 0.5 mm. (ii) Using the maximum variation of brightness in the first n images, $B_n(x,y)\equiv \sup_{i\leqslant n} b_i(x,y) - \inf_{i\leqslant n} b_i(x,y)$, $F(t)$ was defined as the fraction of the region in which $B_n(x,y)$ exceeded a threshold B_{th}. In this paper, we use the threshold $B_{th}\equiv(2/3)\langle B_n^2\rangle/\langle B_n\rangle$, where the symbol $\langle\cdot\rangle$ represents the average over (x,y) and over all images in each experiment. If the coefficient 2/3 is replaced with another value in the range $[1/2,5/6]$, our main results remain the same, although the values of $F(t)$ change accordingly.

Figure 4 shows typical examples of $F(t)$ for various densities, where r is the dilution ratio of the suspension used in these experiments and the time is represented on a logarithmic scale. $F(t)$ increases from zero (the bottom) towards 1 (the top surface). We observe that the form of $F(t)$ does not depend significantly on the experimental conditions although $F(t)$ is translated along the logarithmic time axis.

TABLE I. A summary of the experiments and their results. *O* denotes a front propagation toward the open surface. *H* indicates that the horizontal propagation is observed in some cases, although it is difficult to observe the vertical propagation. + indicates that bioconvection occurs persistently. - indicates that a front propagation or bioconvection is not observed.

Container	Environment	Front propagation	Bioconvection
Cylindrical container	air	*H*	+
Hele-Shaw cells placed vertically	air	*O*	+
	air $\rightarrow$ N_2	*O*	—
	N_2 $\rightarrow$ air	—	+
Hele-Shaw cells placed horizontally or upside down	air	*O*	—

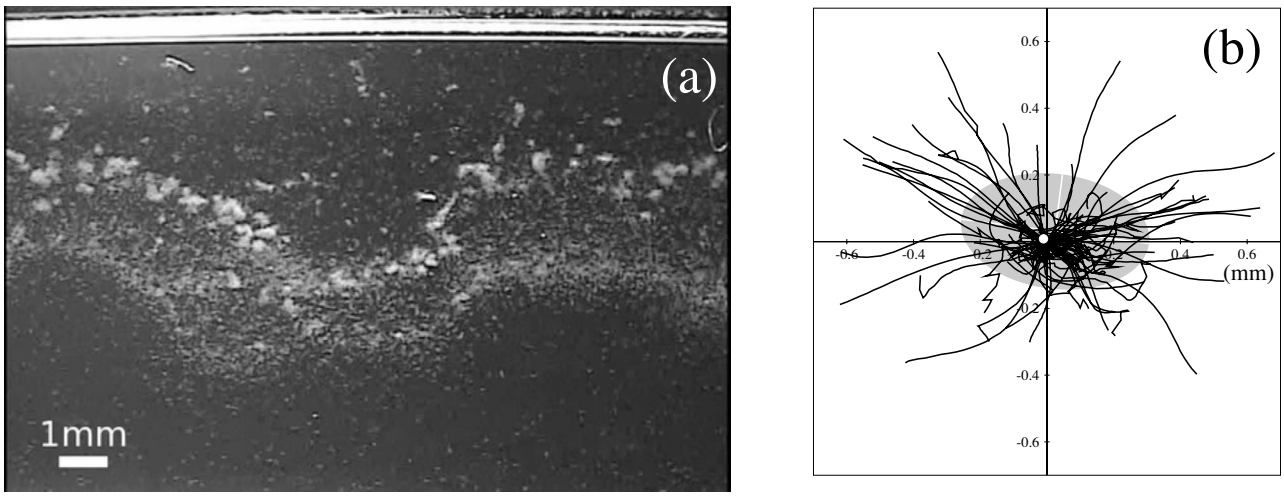

FIG. 9. A front propagating in the Hele-Shaw cell placed horizontally. A suspension with $n_0=1.1\pm0.2$ (10^5 cells/ml) and $V=1.00$ ml was used. (a) A microscopic image of a front. A wire with a diameter 0.3 mm was placed along the water-air interface. (b) Individual trajectories after the passage of the front. They were obtained by the same method as those in Fig. 7(b).

The $F(t)$ values obtained in our experiments were fitted to the function $a/\{1+(\tau/t)^c\}$, which is $a(1+\tanh x)/2$ with the logarithmic time scale $x\equiv c(\ln t-\ln \tau)/2$, using the Levenberg-Marquardt method [55]. Figure 4 shows that the fit is very good. The fitted parameters a and c are insensitive to n_0 and V, and their values are $a=0.92\pm0.1$ and $c=3.1\pm0.8$. The other fitted parameter τ represents the characteristic time for the formation and propagation of the front and changes significantly with both n_0 and V. The characteristic time τ is a decreasing function of n_0, as indicated in Fig. 5(a). The front starts propagating a few minutes after the initial stirring for $n_0=2\times10^5$ cells/ml, while we must wait for more than 1 h to observe the front for 2×10^4 cells/ml. We cannot confirm whether there is a lower threshold density for front formation. Figure 5(b) shows the dependence on the volume of the suspension. For low densities τ decreases with an increase in the depth of the suspension, while it is approximately constant for a very large density.

These results indicate that the front propagation process is approximately characterized by a single time scale that depends significantly on the density of paramecia and the depth of the suspension.

IV. TIME DEVELOPMENT OF CONVECTION

Several descent flows develop to form the roll structures of the fluid convection below the front. We infer that, as in typical bioconvection phenomena, the basic mechanism in the bioconvection of *P. tetraurelia* is analogous to the RT instability [8–10] because the concentration of paramecia causes the suspension in the front to be more dense than the fluid below. In fact, the bioconvection disappears if we turn the container sideways, as reported in Sec. V. The descent flows that develop beneath the front are 4–6 mm away from the neighboring descent flows. This distance is approximately the same as that estimated for other ciliates such as *Tetrahymena* [5,8–10].

In this section we focus on the individual motions of paramecia and the time development of the bioconvection patterns.

A. Movement of paramecia

Figure 6(a) shows a microscopic image of a front. Figures 6(b) and 6(c) show space-time plots, each of which is constructed from the series of images by concatenating a sequence of columns of pixels sliced at a fixed horizontal position. The horizontal positions in Figs. 6(b) and 6(c), indicated by black arrows in Fig. 6(a), are in an upward flow and a descent flow, respectively. Paramecia are advected with random movement in the descent flows, while they swim upward in regions outside these descent flows.

Paramecia combine to produce clusters containing several or dozens of individuals in the front. These clusters stop at a wall of the container or move randomly with velocities that are significantly less than the swimming speed of a single paramecium. They are subsequently carried away from the front by the descent flows. Paramecia swim separately in the upward flows because the clusters are disassembled in the descent flows. Although some clusters often drop away from the front into the upward flows, the front is stable against such disturbance if the number of dropped clusters is small. A single cluster falling in the upward flows is disassembled quickly, as shown in Fig. 6(b), and the constituent individuals swim back to the front.

We investigated the individual motions of paramecia before and after the passage of the front by observing at a fixed position in the Hele-Shaw cell. Figures 7(a) and 7(b) show the trajectories of paramecia for a duration of 1 s, where all trajectories are translated to begin from the origin. In each figure, 100 paramecia in the microscopic images are selected randomly, although clusters that are larger than 3 times the

area of a single paramecium are removed in our analysis.[3] The gray ellipse and its center represent the covariance ellipse and the average of these displacements of paramecia. The fluid velocity in the suspension can be estimated from the movement of small, passive, suspended particles carried by the fluid flow. The average of the displacements of 100 passive particles for 1 s is indicated by a small white circle in each figure. In this analysis, particles whose size is less than half that of a paramecium are considered as passive particles. Neither fluid flow nor the directional swimming of paramecia occurs until the passage of the front. Paramecia move randomly or stop at the walls, while some of them form small aggregates and sink gradually. After the passage of the front, paramecia swim in the upward direction with a velocity that is several times that of the flow of the ambient fluid, as shown in Fig. 7(b).

B. Spatiotemporal patterns of bioconvection

Bioconvection is sustained for at least several hours after the front stops propagating beneath the surface. Figure 8 shows the space-time plots of horizontal slices for three experiments; they are constructed for a given height y. The ordinate axis represents the time after stirring. The density of paramecia is almost uniform after stirring until the pattern of bioconvection appears with the passage of the front. Bioconvection is typically found to form nonstationary structures, as shown in Fig. 8(b). New descent flows develop frequently beneath the front and then move to coalesce into large flows. Figures 8(a) and 8(c) show that the structures of bioconvection change with the depth of the suspension and the density of paramecia in different ways. Bioconvection settles in a virtually stationary structure as the depth decreases, as shown in Fig. 8(a). In contrast, Fig. 8(c) shows that the nonstationary structures are maintained with a decrease in the density, although the time development of the roll structures is decelerated.

In the nonstationary structures of *P. tetraurelia*, as shown in Figs. 8(b) and 8(c), the descent flows develop into large flows at an interval which is of the same order as the depth of the suspension. On the contrary, the spacing of the descent flows emerging beneath the front does not appear to depend significantly on the depth of the solution or the height of the front, as shown in Fig. 3 and Figs. 8(a) and 8(b). Thus there are two characteristic lengths in the bioconvection of *P. tetraurelia*: the depth of the suspension and the instability length of the front. We conjecture that the discrepancy between these two characteristic lengths causes the nonstationary structures.

The coalescence of the descent flows has been reported in numerical simulations conducted by Harashima *et al.* Their mathematical model for the bioconvection of *Heterosigma akashiwo* assumes that individual microorganisms swim upward at a constant velocity [30]. In their simulations, the bioconvection approaches a stationary structure or an intermittent state due to such coalescence. Thus it is possible that feedback from bioconvection with a size of the depth of suspension causes the selection of descent flows through coalescence. By assuming that the front is destabilized through a mechanism analogous to the RT instability, it is inferred that the instability length depends on the density difference created by the front [8–10]. In order to justify our conjecture, we need to clarify the front formation process.

V. CAUSE OF FRONT FORMATION

We performed several experiments as listed in Table I to investigate the cause of front formation.

A. Role of gravity

Paramecium is known to show the negative gravitaxis in darkness and the positive gravitaxis in light [46], and the sign of gravitaxis also depends on the oxic condition [16]. In our experiments, oriented swimming in the upward direction does not occur until passage of the front, as mentioned in the previous section. Therefore tactic responses are not considered to occur before front formation.

In order to decide whether gravity plays a major role, we turned the Hele-Shaw cells sideways and upside down. A thin stainless-steel wire was inserted along the water-air interface to keep it straight. Figure 9(a) shows a microscopic image of a front in the horizontal case. In fact, the front appeared and propagated toward the water-air interface even when the Hele-Shaw cell was placed horizontally or turned upside down, although no pattern of fluid convection appears behind the front. These results indicate that gravity is responsible for the bioconvection, but not for the front formation in suspensions of *P. tetraurelia*.

The horizontal case also differs from the vertical case in terms of the individual motions after the passage of the front. Figure 9(b) shows individual trajectories after the passage of the front, which were extracted by the same method as those in Fig. 7(b). There is no directional flow of paramecia, although they swim as actively as in the vertical case. Thus negative gravitaxis is not responsible for the front formation of *P. tetraurelia* although, in the vertical case, it may play some role in the upward swimming after the passage of the front.

B. Experiments in the nitrogen environment

Paramecia are known to exhibit oxykinesis, and therefore they are attracted to the region of aeration [47,49]. We conducted experiments in a nitrogen environment to investigate the effect of air on bioconvection. The Hele-Shaw cell was placed vertically in an airtight container after stirring, and then the air in the container was replaced with nitrogen gas. Figure 10 shows a series of images obtained in the experiment. The front propagated upward even after the replacement, as shown in the second image from the bottom. However, the front dissipated with bioconvection as soon as it reached the top surface, and the density of paramecia became uniform in the suspension. After nitrogen was replaced with air again, paramecia gathered beneath the top surface and several descent flows developed to recover bioconvection. In

[3]We used the image processing software ImageJ (http://rsb.info.nih.gov/ij/) and its plugin MTrack2.

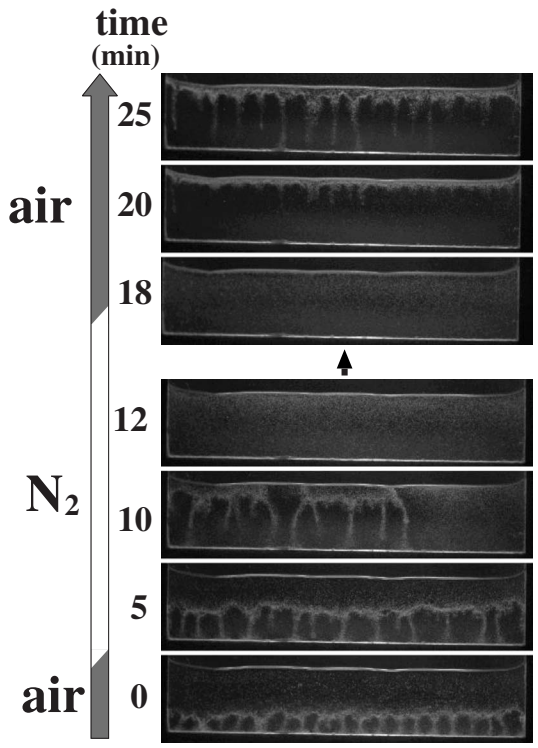

FIG. 10. Results of an experiment conducted in the nitrogen environment. A suspension with $n_0=0.61\pm0.22$ (10^5 cells/ml) and $V=1.00$ ml was used. The environment in which each image was obtained is indicated on the left side.

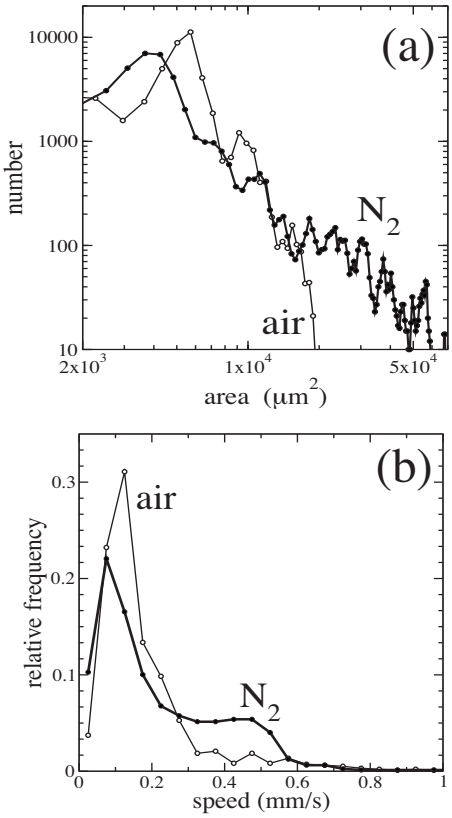

FIG. 11. Individual motions of paramecia in the air and nitrogen environments. We used a diluted suspension with $n_0=0.048\pm0.007$ (10^5 cells/ml) and $V=0.80$ ml. (a) Size distribution of clusters and (b) distribution of swimming speed.

this case, it should be noted that the front propagation did not occur and the fluid convection developed in a manner similar to that of typical bioconvection phenomena.

Next we compared the individual motions of paramecia in the air and nitrogen environments. We placed a low-density suspension in the cylindrical container and observed horizontal movements of paramecia with a microscope from the top. In both environments, paramecia swam actively for a few minutes after initial stirring. However, in the air environment, most of the paramecia slowed down and ceased to swim individually. In contrast, in the nitrogen environment, paramecia continued to swim actively, while some of them collided to form clusters. Paramecia kept swimming actively for more than at least 15 min in this experiment although they are aerobic organisms. We inferred that the paramecia were consuming oxygen remaining in the suspension.

We analyzed 5 s of video images obtained 4 min after stirring by the same method as that in Fig. 7. Figures 11(a) and 11(b) show the distributions of the cluster size and swimming speed. The cluster sizes were derived from the area of a cluster in the images, and the peak in each size distribution corresponds to the area of a paramecium. It should be noted that speeds in the range of 0.3–0.6 mm/s were more frequent in the nitrogen environment than in the air environment.

C. Discussion

An increase of the swimming velocity of *P. aurelia* under low-oxic conditions has been reported in experiments on gravitaxis [16]. It is also known that a large increase of the swimming speed in *Paramecium* is associated with the strong repellent action in chemokinesis [49].

An increase in activity is also observed after the passage of the front, as shown in Figs. 7(b) and 9(b). The results of the nitrogen experiments suggest that front formation by *P. tetraurelia* is caused by a lack of oxygen dissolved in the suspension. Paramecia consume oxygen in the suspension, and a lack of oxygen makes their swimming active. The dependence of the front formation time on the density and the depth, as reported in Sec. III, is consistent with this mechanism. It is inferred that the lack of oxygen first appears in the vicinity of the bottom because oxygen is supplied from the water-air interface. Even when air is replaced with nitrogen, paramecia that comprise the front may not detect the fact until the front comes close to the interface because oxygen diffuses slowly in the stationary suspension above the front. On the other hand, when nitrogen is again replaced with air, it is expected that the paramecia gather beneath the surface without exhibiting front propagation because oxygen in the suspension is already low.

Bioconvection induced by the lack of oxygen has been reported for some kinds of bacteria [3,4,6,12]. The delay time for pattern formation is significantly dependent on the average cell concentration as observed in our experiments. However, in those cases, oxykinesis causes directional flows of bacteria due to a steep gradient in the oxygen concentra-

tion and a high-density layer appears at the outset beneath the top surface, not in the vicinity of the bottom. It may be caused by nonlinear responses to oxygen [47,49], as in the competing responses of *D. desulfuricans* bacteria, which has both positive and negative responses to oxygen depending on its concentration [6]. An important difference between paramecia and bacteria is that the mean free path of paramecia is much larger than that of bacteria. In our systems the mean free path of paramecia below the front is larger than or approximately equal to the front thickness. Therefore we should consider oxykinesis as a microscopic behavior rather than the macroscopic response to an oxygen gradient. The unoriented swimming observed behind the front in the horizontal container is consistent with the inference that the individual response is kinetic.

There may be a mechanism responsible for the sharpness of the front. It is inferred that cell-cell interactions are important because the diffusion of paramecia in dilute suspensions is too fast to form a sharp front. Paramecia collide with each other and form clusters when they enter the front. Such behavior is analogous to a traffic jam. Collisions in high-density states can play a major role in front formation, as indicated by the clustering phenomena of driven granular gases [56,57]. In order to clarify these mechanisms, it is necessary to experimentally measure both the distribution of the oxygen concentration and the density of paramecia.

In our experiments, the upward swimming of paramecia appears after the passage of the front only when the Hele-Shaw cells are placed vertically. *P. aurelia* is known to show negative gravitaxis as the oxygen concentration decreases [13,16,17]. Negative gravitaxis is not a necessary factor for front formation because the front also occurs in a horizontal container. However, it possibly enhances front formation and bioconvection in a vertical Hele-Shaw cell.

VI. CONCLUSIONS

We investigated bioconvection in high-density suspensions of *P. tetraurelia*. In the experiments conducted using Hele-Shaw cells placed vertically, we found that bioconvection began as a high-density front propagating from the bottom toward the water-air interface. The formation and propagation of the front required a long time when either the density of paramecia or the depth of the suspension decreased. In nitrogen environments, the front dissipated. We confirmed that paramecia become active with the passage of the front and similar activity is induced by the lack of air. These results suggest that paramecia consume oxygen dissolved in the suspension and that a lack of oxygen causes the front formation.

Front propagation appeared even in a Hele-Shaw cell placed horizontally, but the oriented swimming of paramecia was not observed. Therefore oxykinesis appears to be essentially responsible for front formation. Negative gravitaxis may play a role in enhancing bioconvection because oriented swimming was observed below the front in the vertical case.

Paramecia combined to form clusters in the front. Although descent fluid flows advect paramecia from the front, the crowded front was maintained by the upward swimming of individuals returning to the front. Cell-cell interactions such as collisions are important at such high densities and may be responsible for the sharpness of the front.

The bioconvection of *P. tetraurelia* produces nonstationary roll structures as the depth of the suspension increases. The spacing of the descent flows emerging from the front does not depend significantly on the depth, while they coalesce to form large flows at intervals of the order of the depth. We conjecture that the inconsistency between the instability length of the front and the depth of the suspension causes the nonstationary structures. The development of a mathematical model for front formation is a problem which will be addressed in the future.

ACKNOWLEDGMENTS

The authors are very grateful to Y. Takagi for providing equipment and technical advice and for discussing our results with considerable interest. We thank K. Ishii and J. Karimata for providing the apparatus for the nitrogen experiments and C. Urabe for fruitful discussions.

[1] J. R. Platt, Science **133**, 1766 (1961).
[2] M. A. Bees and N. A. Hill, J. Exp. Biol. **200**, 1515 (1997).
[3] I. M. Jánosi, J. O. Kessler, and V. K. Horváth, Phys. Rev. E **58**, 4793 (1998).
[4] A. Czirók, I. M. Jánosi, and J. O. Kessler, J. Exp. Biol. **203**, 3345 (2000).
[5] Y. Mogami, A. Yamane, A. Gino, and S. A. Baba, J. Exp. Biol. **207**, 3349 (2004).
[6] J. P. Fischer and H. Cypionka, FEMS Microbiol. Ecol. **55**, 186 (2006).
[7] R. N. Bearon and D. Grünbaum, Phys. Fluids **18**, 127102 (2006).
[8] M. S. Plesset and C. G. Whipple, Phys. Fluids **17**, 1 (1974).
[9] S. Childress, M. Levanodowsky, and E. A. Spiegel, J. Fluid Mech. **63**, 591 (1975).
[10] M. S. Plesset, C. G. Whipple, and H. Winet, J. Theor. Biol. **59**, 331 (1976).
[11] T. J. Pedley and J. O. Kessler, Annu. Rev. Fluid Mech. **24**, 313 (1992).
[12] N. A. Hill and T. J. Pedley, Fluid Dyn. Res. **37**, 1 (2005).
[13] D.-P. Häder, P. Richter, M. Ntefidou, and M. Lebert, Adv. Space Res. **36**, 1182 (2005).
[14] P. R. Richter, M. Ntefidou, C. Streb, J. Faddoul, M. Lebert, and D.-P. Häder, Acta Protozool. **41**, 343 (2002).
[15] M. Lebert and D.-P. Häder, Nature (London) **379**, 590 (1996).
[16] R. Hemmersbach-Krause, W. Briegleb, and D.-P. Häder, Eur. J. Protistol. **27**, 278 (1991).
[17] D.-P. Häder, Adv. Space Res. **24**, 843 (1999).
[18] R. Bräucker, S. Machemer-Röhnisch, and H. Machemer, J. Exp. Biol. **197**, 271 (1994).

[19] M. Krause, R. Bräucker, and R. Hemmersbach, Protoplasma **229**, 109 (2006).
[20] J. O. Kessler, Nature (London) **313**, 218 (1985).
[21] A. M. Roberts, Biol. Bull. **210**, 78 (2006).
[22] J. O. Kessler, Comments Theor. Biol. **1**, 85 (1989).
[23] T. J. Pedley and J. O. Kessler, J. Fluid Mech. **212**, 155 (1990).
[24] S. Ghorai and N. A. Hill, Bull. Math. Biol. **62**, 429 (2000).
[25] S. Ghorai and N. A. Hill, J. Theor. Biol. **219**, 137 (2002).
[26] I. M. Jánosi, A. Czirók, D. Silhavy, and A. Holczinger, Environ. Microbiol. **4**, 525 (2002).
[27] S. Ghorai and N. A. Hill, Phys. Fluids **17**, 074101 (2005).
[28] J. O. Kessler, J. Fluid Mech. **173**, 191 (1986).
[29] T. J. Pedley, N. A. Hill, and J. O. Kessler, J. Fluid Mech. **195**, 223 (1988).
[30] A. Harashima, M. Watanabe, and I. Fujishiro, Phys. Fluids **31**, 764 (1988).
[31] N. A. Hill, T. J. Pedley, and J. O. Kessler, J. Fluid Mech. **208**, 509 (1989).
[32] A. M. Metcalfe and T. J. Pedley, J. Fluid Mech. **370**, 249 (1998).
[33] M. M. Hopkins and L. J. Fauci, J. Fluid Mech. **455**, 149 (2002).
[34] M. Nagataki, in *Analysis of Nonlinear Phenomena: Experiments and Mathematical Analysis*, edited by M. Nagayama, Vol. 1313 of *RIMS Kokyuroku* (RIMS, Kyoto, 2003), pp. 36–46 (in Japanese).
[35] S. Fujita and M. Watanabe, Physica D **20**, 435 (1986).
[36] Z. Alloui, T. H. Nguyen, and E. Bilgen, Int. Commun. Heat Mass Transfer **32**, 739 (2005).
[37] A. Bahloul, T. Nguyen-Quang, and T. H. Nguyen, Int. Commun. Heat Mass Transfer **32**, 64 (2005).
[38] X.-L. Wu and A. Libchaber, Phys. Rev. Lett. **84**, 3017 (2000).
[39] T. Vicsek, A. Czirók, E. Ben-Jacob, I. Cohen, and O. Shochet, Phys. Rev. Lett. **75**, 1226 (1995).
[40] G. Grégoire and H. Chaté, Phys. Rev. Lett. **92**, 025702 (2004).
[41] N. H. Mendelson, A. Bourque, K. Wilkening, K. R. Anderson, and J. C. Watkins, J. Bacteriol. **181**, 600 (1999).
[42] K. Watanabe, J. Wakita, H. Itoh, H. Shimada, S. Kurosu, T. Ikeda, Y. Yamazaki, T. Matsuyama, and M. Matsushita, J. Phys. Soc. Jpn. **71**, 650 (2002).
[43] C. Dombrowski, L. Cisneros, S. Chatkaew, R. E. Goldstein, and J. O. Kessler, Phys. Rev. Lett. **93**, 098103 (2004).
[44] S. Kitsunezaki, Physica D **216**, 294 (2006).
[45] S. Kitsunezaki, in *Mathematical Aspects of Complex Fluids and their Applications*, edited by O. Sano, Vol. 1472 of *RIMS Kokyuroku* (RIMS, Kyoto, 2006), pp. 129–138 (in Japanese).
[46] H. M. Fox, Proceedings of the Cambridge Philosophical Society. Biological Sciences **1**, 219 (1925).
[47] R. Wichterman, *The Biology of Paramecium*, 2nd ed. (Plenum Press, New York, 1986).
[48] J. V. Houten and J. V. Houten, J. Theor. Biol. **98**, 453 (1982).
[49] J. V. Houten and R. R. Preston, in *Paramecium*, edited by H. D. Görtz (Springer, Berlin, 1988), pp. 282–300.
[50] K. Hausmann and N. Hülsmann, *Protozoology*, 2nd ed. (Georg Thieme Verlag, New York, 1996).
[51] Y. Takagi, K. Nimura, Y. Tokusumi, H. Fujisawa, and K. Kaji, Zoolog Sci. **13**, 89 (1996).
[52] Y. Tokusumi and Y. Takagi, Zoolog Sci. **17**, 341 (2000).
[53] N. Mizobuchi, K. Yokoigawa, T. Harumoto, H. Fujisawa, and Y. Takagi, J. Eukaryot Microbiol. **50**, 299 (2003).
[54] A. Miyake, in *Sexual Interaction in Eukaryotic Microbes*, edited by D. H. O'Day and P. A. Horgen (Academic Press, New York, 1981), pp. 95–129.
[55] W. H. Press, B. P. Flannery, S. A. Teujiksky, and W. T. Etterling, *Numerical Recipes* (Cambridge University Press, New York, 1997).
[56] Y. Du, H. Li, and L. P. Kadanoff, Phys. Rev. Lett. **74**, 1268 (1995).
[57] *Granular Gas Dynamics*, edited by T. Pöschel and N. Brilliantov, Vol. 624 of *Lecture Notes in Physics* (Springer, Berlin, 2003).